Structures 47 (2023) 800–813

Contents lists available at ScienceDirect

Structures

journal homepage: www.elsevier.com/locate/structures

An experimental and numerical study of the strengthening of masonry brick vaults

Sukran Tanriverdi *

Department of Civil Engineering, Aksaray University, 68100, Turkey

ARTICLE INFO

Keywords:
Repair
Strengthening
Historical structures
Masonry vaults
FRP
Tie rod

ABSTRACT

Vaults are curvilinear cover systems that cover open spaces formed by the combination of arches. The vaults, built using materials such as stone and brick, are used in historical buildings such as mosques, madrasahs, inns, baths, churches, and monasteries. In this study, experimental studies were carried out to examine the reinforcement techniques with steel and different types of CFRP strip applications applied to masonry vaults. Within the scope of the research, one reference sample, one tie rod, four reinforced CFRP materials of different designs, and a total of six masonry vault samples were tested under axial compression. The test vault samples were also analyzed numerically in the LUSAS Analysis Program, and the test results obtained from the numerical analysis were compared. According to the results obtained, the load-bearing capacity of the reinforced samples increased by at least 45% compared to the non-reinforced sample that was named as the reference.

1. Introduction

Throughout history, people have built historical structures such as bridges, palaces, inns, baths, caravanserais, and mosques on their lands. These structures, which have survived from the past to the present, reflect the technological, economic, and cultural characteristics of the period they were built in. Historical structures are among the masonry building types. Masonry structures have low tensile strength. They are structures that are all or a combination of bearing elements such as arches, vaults, domes, columns, and walls, obtained by combining materials with high compressive strength such as briquettes, bricks, and stones with the help of mortar. Arches, domes, vaults, walls, and columns are the bearing systems of historical buildings.

Vaults are single curvature structural elements formed by arranging the arches one after the other and connecting them. Since they are generally built from materials such as stone and brick, their compressive strength is high and their tensile strength is low. The vaults are divided into eleven different groups according to their geometric shapes. These are barrel vault, high vault, conical vault, cavetto vault, drop vault, pointed vault, curved vault, oblique vault, monastery vault, groin vault, and mulden vault [1]. In this study, the shape of the barrel vault is discussed. In Fig. 1, examples of barrel vaults are given.

Reasons such as insufficient ground conditions, wars, loss of strength of building materials as a result of deterioration over time, errors in design and application, severe earthquakes, and wind loads cause some damage to historical buildings. These structures, which are historical documents, are one of our most important responsibilities and duties to transfer them to future generations and to protect them. In vaults, horizontal forces such as earthquakes are supported by struts, walls, and with the help of tie rods, as in arched structures (Fig. 1b).

Many studies have been carried out on the behavior of structural carrier systems against fixed, live load, earthquake, and wind loads to transfer historical buildings to the future [2–18]. Experimental and theoretical research has also been carried out to determine the behavior of historical buildings reinforced with different materials. In his study, Foraboschi [19] strengthened the inner and outer parts of the arch and vault building elements with FRP (Fiber Reinforced Polymer), designed the hinge mechanism in such a way that it would not create a collapse mode, and examined the behavior of the structure. He presented mathematical models for behavioral patterns such as slipping, crushing, debonding, and FRP rupture. Thanks to the mathematical models obtained as a result of the study, the maximum load-bearing capacities were found for each failure mode. The load-bearing capacities of the reinforced arch and the vault increased by at least 7.8 and 2.1 times, respectively than the load-bearing capacities of the unreinforced arch and vault. Milani and Bucchi [20] developed a kinematic finite element model to determine the failure mechanism and failure load of curved brick structural members such as arches and domes reinforced with

* Corresponding author.
E-mail address: sukrantugrulelci@aksaray.edu.tr.

https://doi.org/10.1016/j.istruc.2022.11.098
Received 11 September 2022; Received in revised form 4 November 2022; Accepted 23 November 2022
Available online 2 December 2022

(a) Suleyman Mosque in Diyarbakır (Turkey) (b) Kurşunlu Han in Uskup (Macedonia)

(c) High Church in Aksaray (Turkey)

Fig. 1. Sample photos of barrel vaults. a) Suleyman Mosque in Diyarbakır (Turkey), b) Kurşunlu Han in Uskup (Macedonia), c) High Church in Aksaray (Turkey).

(a) A1-A6 Sample (b) B1-B6 Sample

Fig. 2. a) Compressive strength test of brick, b) Flexural tensile strength of the bricks.

Table 1
The result of the compressive strength test and flexural tensile strength of the bricks.

Series	Maximum loading (kN)	Compressive strength (N/mm^2)	Series	Maximum loading (kN)	Flexural tensile strength (N/mm^2)
A1	27.98	11.20	B1	8.44	7.12
A2	28.10	11.24	B2	7.64	6.45
A3	31.09	12.43	B3	7.52	6.35
A4	32.64	13.10	B4	8.25	6.96
A5	31.27	12.51	B5	8.12	6.86
A6	33.00	13.20	B6	7.41	6.26
Mean		12.28			6.67
Standard Deviation		0.88			0.36

*A1-A6: Compressive strength of bricks.
*B1-B6: Flexural tensile strength of the bricks.

fiber-reinforced polymer (FRP) strips. They stated that the failure load and failure mechanism of this developed model remained within safe limits and this developed model could be used in practice. Fırat and Eren [21] used FRP in different ways in their studies and they carried out strengthening studies on arch models. As a result of the study, it was determined that the reinforced sample increased its capacity by at least 158 % compared to the unreinforced sample. Ural et al. [22] conducted experimental and numerical studies to examine the effect of different types of tie rods on arch samples. As a result of the study, they determined the tie rod model that should be applied in historical arched structures. Carozzi et al. [23] carried out an on-site experimental study by reinforcing the vaults and arches of a historical building in Italy with composite materials such as FRP, TRM (Textile Reinforced Grout), and SRG (Steel Reinforced Grout). In the experimental study carried out by applying loads in the vertical direction, the load-bearing capacity, stiffness, ductility conditions, and damage modes of reinforced arches and vaults were compared with those of unreinforced arches and vaults. As a result of the strengthening work, it was observed that the load-bearing capacity of arches and vaults increased 4 times with SRG and FRP materials, and 5.5 times with TRM material. De Santis et al. [24] conducted an experimental study on examples of vaults equipped with buttresses and infills, one without reinforcement and three reinforced with SRG. As a result of the study, it was determined that SRG material increased the bearing capacity of the vault 2–3 times by preventing damage. Hamdy et al. [25] strengthened the masonry walls and vaults with different materials and analyzed them in the ANYS program. Mortar, mild steel rods, FRP, Ferrocement ready-made wire, and polyester mortar were used as the reinforcement method. It was determined

(a) C1-C6 Sample (b) D1-D6 Sample

Fig. 3. a) Compressive strength test of mortar, b) Flexural tensile strength of the mortar.

Table 2
The result of the compressive strength test and flexural tensile strength of the mortar.

Series	Maximum loading (kN)	Compressive strength (N/mm^2)	Series	Maximum loading (kN)	Flexural tensile strength (N/mm^2)
C1	7.35	2.94	D1	0.22	0.55
C2	7.24	2.89	D2	0.20	0.50
C3	6.98	2.79	D3	0.20	0.50
C4	7.16	2.86	D4	0.18	0.45
C5	7.20	2.88	D5	0.23	0.58
C6	7.72	3.08	D6	0.21	0.53
Mean		2.91			0.52
Standard Deviation		0.09			0.05

*C1-C6: Compressive strength test of mortar.
*D1-D6: Flexural tensile strength of the mortar.

that the load-bearing capacity of the models made with FRP materials increased more than the other materials. The load-bearing capacity of the vault reinforced with FRP material increased by 190 % compared to the load-bearing capacity of the non-reinforced vault. According to Zampieri et al. [26] analyzed arch samples reinforced with different composite materials using experimental tests. They investigated the effects of reinforcement techniques on the arch structure. De Santis et al. [27] conducted an experimental study on masonry vaults reinforced with BTRM (Basalt Textile Reinforced Mortar) supported by buttresses and infills. Vertical load was applied on the filling in 1/3 span. It was determined that the reinforcement methods delayed the formation of cracks and increased the load-bearing and bending capacity. Varro et al. [28] carried out experimental and analysis studies to examine the behavior of CFRP (Carbon Fiber Reinforced Polymer) reinforced and non-reinforced arched structures. The differences between the bearing capacities and damage types of arched structures were investigated. Alejo Guerra [29] the temple of San Agustin in the city of Morelia, which is recognized as a cultural heritage by UNESCO, was discussed. Dynamic tests of the church were made and its numerical model was developed in the DIANA program. The analysis of the church was made by applying

Table 3
Compressive strength test results of masonry wall samples.

Sample No	Maximum load V (kN)	Compressive strength f (MPa)	Young's modulus E (MPa)	Ratio E/ f_k
Experiment-1	123.55	3.52	2011	632
Experiment-2	144.61	4.12	2060	648
Experiment-3	132.67	3.78	1622	510
Mean	133.61	3.81	1897	596
f_k = f/1.2		3.18		

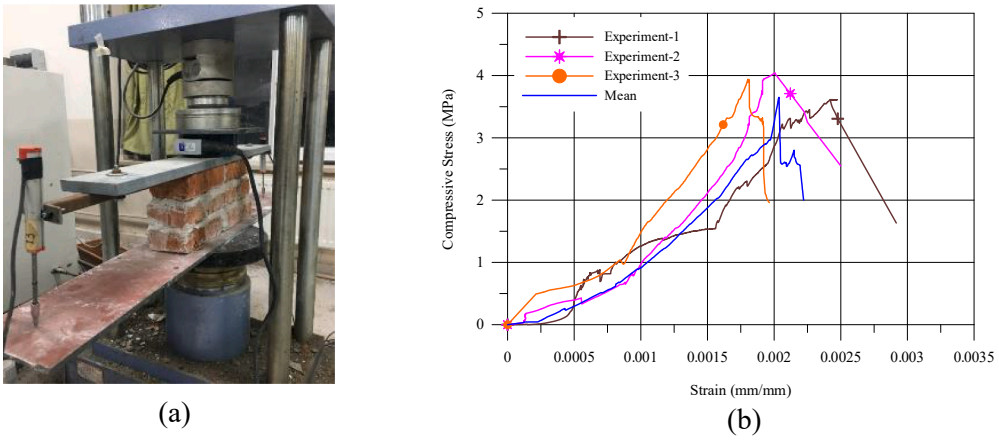

(a) (b)

Fig. 4. a) masonry wall samples compressive strength test, b) Masonry wall samples stress-strain plots.

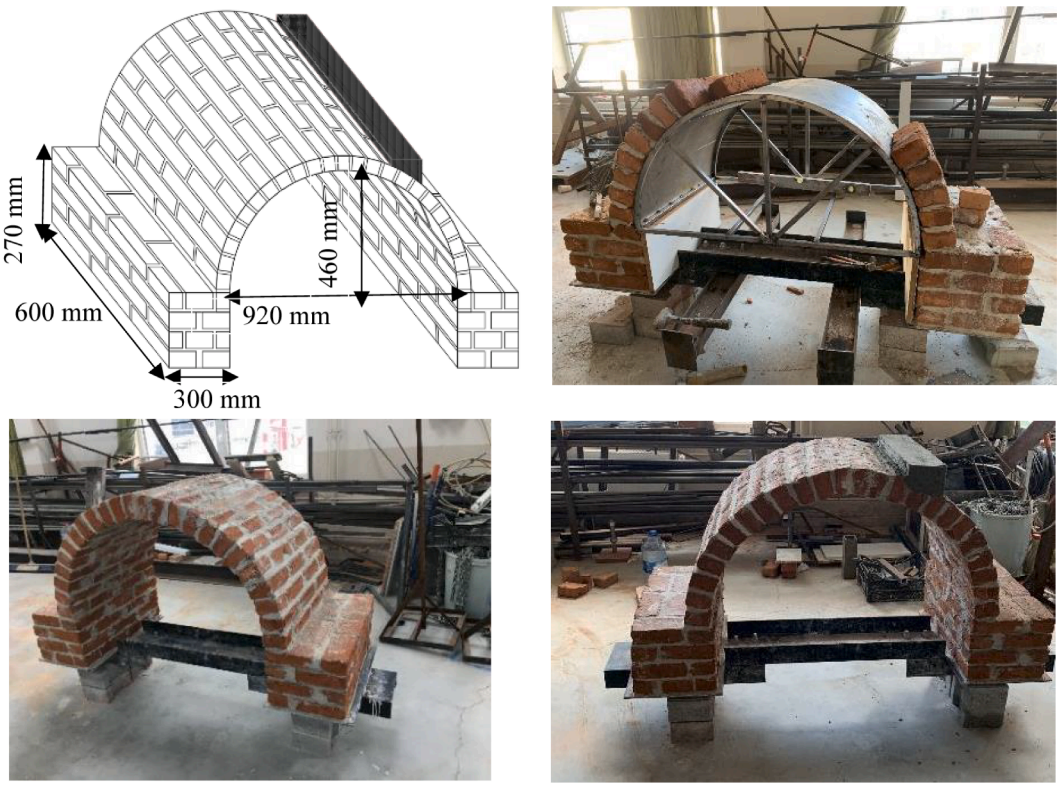

Fig. 5. The general geometry of the vault samples and the construction stages.

reinforcement methods with materials such as steel and TRM on the elements such as the dome, arch, and barrel vault in the church. As a result of the analysis, it was seen that the strengthening techniques provided a maximum increase of 92 % in the capacity of the structure. Siha and Zhou [30] investigated experimentally and theoretically how the reinforcement of historic wooden columns with CFRP and steel bars affects the ductility and bearing capacity of wooden columns. Fırat and Sancar [31] studied the effects of different types of tie rods used at the stone arches. In their study, one reference sample without a tie rod and 6 test samples with a tie rod fixed in different ways were tested. Numerical analyzes of the test samples were also made and compared with experimental results. The samples with tie rods carried at least 1.70 times more load than the reference sample.

Although the unit cost of CFRP is high, it can provide a cost advantage due to the easy workmanship and the low amount used in structural members strengthened. The difficulty of applying heavy materials such as steel can create considerable problems in strengthening works. However, CFRP, which is a lightweight material compared to other reinforcement materials such as steel, has ease of application. In addition, CFRP, which has good resistance to high tensile stresses, does not have corrosion problems. For this reason, besides the steel tie rod, CFRP was also used in the study. In the study, the effects of CFRP and tie rods used in the repair and strengthening of historical buildings on the vaults were investigated experimentally and numerically. A total of six vault samples, one of which was strengthened by using a reference sample without any reinforcement method, with a tie rod, and four using CFRP material in different shapes, were tested in a laboratory environment by applying a load under axial pressure. A numerical analysis of the samples subjected to the test was made and the results were presented by comparing them with each other. In line with the results, it was determined what methods should be applied in strengthening works in the vaults.

2. Material and properties

To determine the mechanical properties of the mortar and brick used in the experimental study, experiments were carried out in Aksaray University, Faculty of Engineering, Civil Engineering, Construction Mechanics laboratory as specified in the standards. Compressive strength tests and flexural tensile strength tests were carried out for the brick used in the vaulted models. Compressive strength tests and flexural tensile strength tests of the mortar used in the horizontal and vertical joints of the masonry units were carried out. In addition, compressive strength tests of the masonry wall samples were carried out to determine the modulus of elasticity to be used in the numerical modeling of the vault models.

2.1. Properties of brick

In the experiments, bricks with the dimensions of 50x90x190 mm^3 were used as a masonry unit. Compressive strength tests and flexural tensile strength tests were carried out to determine the mechanical properties of bricks used in the construction of the vaulted samples. For the compressive strength tests of the bricks, the compressive strength tests were carried out on a total of six bricks with the dimensions of 50x50x30 mm^3, as specified in EN 772–1-2011 + AI [32]. Basing strength values were obtained by dividing the maximum loads obtained as a result of the tests by the applied area. The average compressive strength of the bricks was 12.28 MPa.

Flexural tensile strength tests of masonry units were carried out considering EN 772-6 [33]. Six brick samples were carried out as specified in the standard. The flexural tensile strength of the brick samples was calculated according to Eq. (1) below. The flexural tensile strength of the masonry units was obtained on average 6.67 MPa. The test image for the compressive strength and flexural tensile strength tests of the brick is given in Fig. 2.

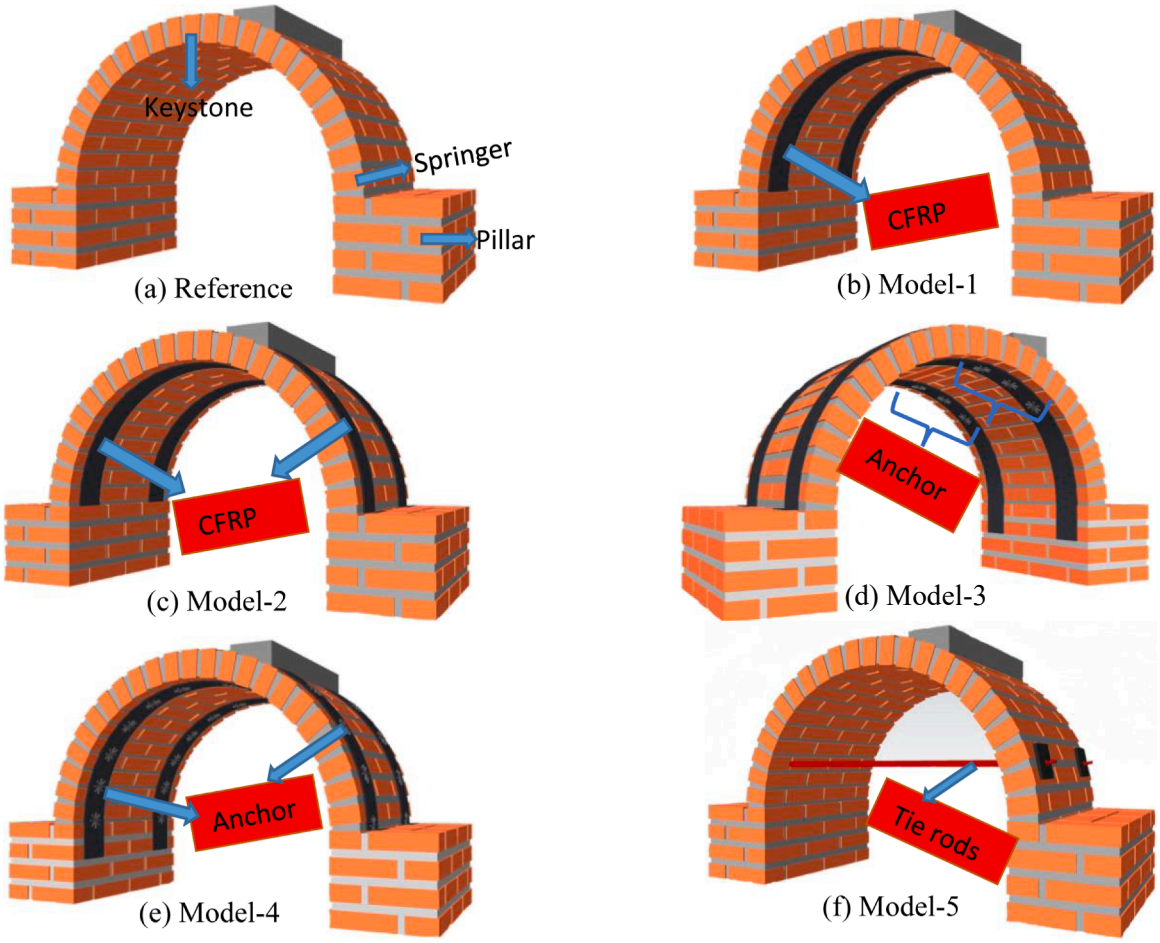

Fig. 6. Drawings of vault samples.

$$R_{tf} = \frac{PL}{bd^2} \quad (1)$$

where R_{tf} is the flexural tensile strength (N/mm^2), P represents the maximum loading (N), b (mm) is the width of the brick, d (mm) is the height of the brick, and L (mm) is the length of the brick. Compressive strengths of masonry units are expressed from A1 to A6, and flexural tensile strengths are expressed from B1 to B6. In Table 1, the test results for the compressive and flexural tensile strength of the bricks are given collectively.

2.2. Properties of Khorasan mortar

Khorasan mortar was used for vault sample lining. The ratios of mortar in sand/lime/stone dust are 4/4/2 by volume. As specified in EN 12390-3 [34] standard, compressive strength tests were carried out on six mortar samples with dimensions of 50 × 50 × 50 mm^3. The compressive strength values of the samples are the value obtained by dividing the maximum load obtained by the applied area. As a result of the experiment, the average compressive strength of the mortar was 2.91 MPa.

EN 12390-6 [35] standards were taken into account for determining the flexural tensile strength of Khorasan mortar samples. Six mortar samples of 40 × 40 × 160 mm^3 were subjected to testing. The flexural tensile strengths of the mortar samples were calculated with the help of Eq. (1) as specified in EN 12390-6 [35]. The compressive strength of the mortar is symbolized from C1 to C6, and the flexural tensile strength in bending is symbolized from D1 to D6. Compressive and flexural tensile strength tests of Khorasan mortar are given in Fig. 3 and the results are given in Table 2. As seen in Table 2, the average flexural tensile strength of the mortar is 0.52 MPa.

2.3. Properties of tie rod

In the experiment, a tie rod cut from sheet metal with a thickness of 3 mm and a width of 20 mm was used. EN ISO 6892-1 [36] standard was taken into account to determine the tensile strengths of the tie rod. The tensile strength of the tie rod was calculated as specified in Eq. (2).

$$R_m = F_m \quad (2)$$

R_m is the tensile strength of the tie rod (N/mm^2), and F_m is the maximum load that the test sample withstands after the yield point is passed during the test. The tensile strength of the tie rod was found to be 275 MPa on average [37].

2.4. Compressive strength of masonry wall samples

To determine the modulus of elasticity to be used in the analysis of the vault samples, compressive strength tests were carried out on three wall samples. The wall samples were produced in dimensions of 390 × 190 × 90 mm^3 in accordance with the standard EN 1052-1:1998 [38]. Two LVDTs were placed on the wall samples. The strains occurring in the wall samples during the experiment were calculated. Stress was also obtained by dividing the vertical load applied on the wall samples by the applied area. The compressive strength test of masonry walls and the stress-strain graph of this test are given in Fig. 4 and the test results are given in Table 3 collectively. As stated in EN 1996–1-1 + A1 [39], the ratio of the modulus of elasticity to the compressive strength for each

Fig. 7. Anchorage application, a) Drilling anchor holes, b) Preparation of anchors, c) Placing anchors in holes, d) Completion of anchor applications.

wall sample is less than 1000.

3. Vault test samples

3.1. Preparation of test samples

One non-reinforced and five different reinforced vault test samples with a span of 920 mm, a height of 460 mm, and a width of 600 mm were designed. In the experiment, Khorasan mortar was used for horizontal and vertical joints of brick and masonry units with dimensions of 190 × 90 × 50 mm^3. Joint spacing was 10 mm in the column and 8 mm elsewhere. In this study, the height and span of 20 vaults were measured in total. Their average values were determined, and the dimensions of the test samples were determined by reducing the height and span of the vault by an average of 1/4, taking into account the dimensions of the test apparatus prepared with steel profiles. The depth of the vault was considered to be the maximum according to the test apparatus. The vertical loading was applied to the vault samples. Reinforced concrete was placed in the area where the vertical load was applied (230 mm away from the keystone) so that the applied load does not damage the masonry units in the upper row and the load shows a uniform distribution. To study the behavior of the reinforced brick vaults, a total of six samples were investigated experimentally and numerically under axial loads applied to 1/4 of their span. The vaults were built with bricks arranged in a single skin, therefore their thickness was thin (5 cm). For this reason, to increase the strength of the vaults under axial load, a catenary curve was selected as the directrix of vaults, with coefficients close to the ones of a drop arch [40]. In the experimental study, the bottom ends of the pillars were designed as fully fixed support and the displacements were zeroed. The experimental process was carried out by placing each sample in the experimental setup 28 days after it was produced. The general geometry and construction stages of the vaulted samples are given in Fig. 5. The modeling of the vaults is given in Fig. 6.

No strengthening method was applied in the vault sample, which is called the reference sample. (Fig. 6a). The load and displacements to be carried by the reference sample were accepted as reference. The purpose of making a reference sample was to examine the effect of each strengthening method on the vaulted structures by comparing them with the reinforced samples.

In Model-1, two 100 mm wide CFRP strips were applied to the inside of the vault sample, leaving a 50 mm gap from the edges (Fig. 6b). The surfaces on which CFRP application was made were first cleaned and epoxy resin was applied. CFRP strips cut on the epoxy resin were adhered. In Model-2, the vault sample was reinforced with two 100 mm wide CFRP strips, leaving 50 mm gaps from the inside and outside (Fig. 6c). In Model-3, as in Model-2, the vault sample was strengthened by applying CFRP strips to the inner and outer parts of the vault. Unlike Model-2, CFRP strips were applied on the inner surface of the vault, starting from 150 mm below the springer (Fig. 6d). Three 10 mm diameter anchor holes were drilled in the inner part of the vault, only in the area where the load was applied, at two joint intervals, as shown in Fig. 7a. Anchorage was obtained by wrapping CFRP around a steel bar with a diameter of 8 mm and a length of 40 mm. The hole to be anchored were filled with epoxy resin and the prepared anchors were placed in the holes (Fig. 7c). The part of the anchor consisting only of CFRP was glued onto the CFRP strip by opening it circularly as shown in Fig. 7d.

In Model-4, unlike Model-3, as shown in Fig. 6e, the anchoring process was applied to the inner and outer parts of the vault, leaving gaps of 10 mm in diameter between two joints. In Model-5, tie rods were used as a different material to strengthen the vault. The tie rods were applied from the 60 % lower part of the vault height, where the tensile strength of the vault was formed. The tie rods were removed to the opposite side through the hole drilled on the vault and fixed to the 10 mm thick square section plate with the help of bolts (Fig. 6f). In Fig. 8,

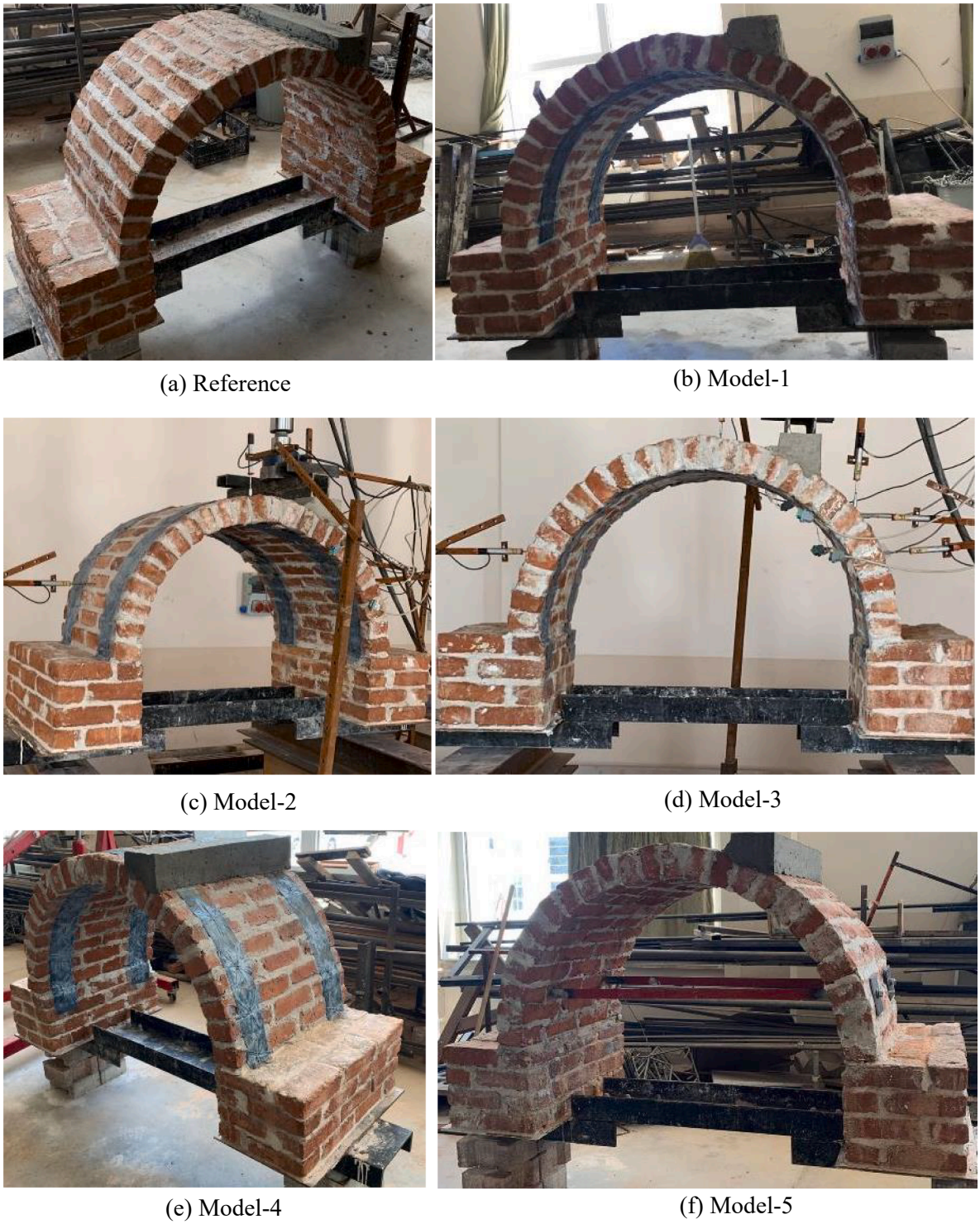

Fig. 8. Pre-experimental images of the samples.

pre-experimental images of all models are given.

3.2. Experimental setup

In the experimental study, the loading was done with the help of a hydraulic jack with a capacity of 100 kN. In the case of applied load, the load cell was exposed to pressure and records by giving a certain stress from the outlet end. The stress taken from the load cell was transferred to the computer thanks to the established mechanism. The experimental set had a load and displacement control system. In the experimental study, the average loading rate was 0.3 kN/*sec* in a load-controlled manner. After the experimental samples reached the maximum load, the displacement control mode was started. The mean displacement value was maintained at 5 mm/*sec*. Horizontal and vertical displacements were measured with Linear Variable Differential Transformers (LVDT) throughout the experimental study. In Fig. 9, the experimental setup and the LVDTs placed in the experimental setup are given.

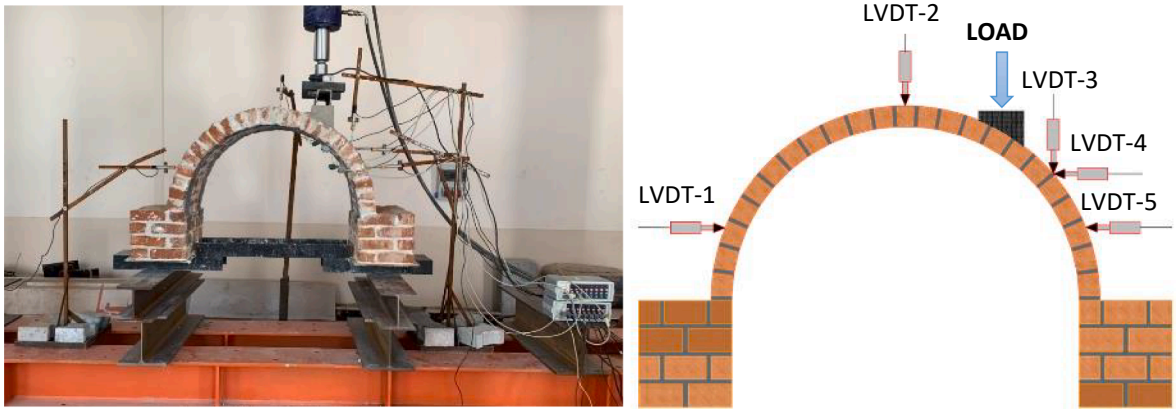

Fig. 9. The experimental setup and the LVDTs placed in the experimental setup.

Table 4
Experimental test results.

Test series	P_f (kN)	Increment[a] (%)	Matched vertical displacement to the maximum load (mm)	Matched horizontal displacement to the maximum load (mm)
Reference	8.381	0	0.186	0.186
Model-1	15.211	81.493	0.762	1.255
Model-2	31.335	273.881	4.110	10.377
Model-3	33.898	304.462	3.727	9.315
Model-4	40.822	387.077	4.850	12.781
Model-5	12.171	45.221	7.973	6.143

[a] Increments of the compressive strength in relation to the reference vault.

3.3. Experiment results

All LVDTs were attached to the same zones on the vault test samples throughout the experiment. In the studies, vertical displacements under maximum load were measured with LVDT-2 placed on the keystone of the vault samples. The horizontal displacements under the maximum load were calculated by calculating the sum of the LVDT-1 and LVDT-5 values placed horizontally on the right and left sides of the vault samples. In the studies, the axial load was applied to the vault samples in the vertical direction. The maximum load obtained in the experiments and the vertical and horizontal displacements corresponding to the maximum load are given in Table 4 and Fig. 10.

When Table 4 and Fig. 10 are examined, as a result of the experimental study, the load-bearing capacity of the reference sample without any reinforcement was measured as 8.381 kN. The first capillary cracks in the reference sample were observed when the load was 3 kN. With the increase in the load, large cracks were observed in the area where the load was applied and in the horizontal joints where the vault arc started in the right part of the vault. As a result of the experiment, hinges were formed in four places, in the right and left parts of the vault, where the load was applied, and in the right part, where the vault arc started. The vertical and horizontal displacement of the reference sample under maximum load was 0.186 mm. Taking into account the cracks in the reference sample, two 100 mm wide CFRP strips were left in the interior of the vault sample by leaving a 50 mm gap from the edges.

This sample, named Model-1, carried a maximum load of 15.211 kN. While the load was at 15.211 kN, the vertical displacement of Model-1 was 0.762 mm and the horizontal displacement was 1.255 mm. Model-1 carried approximately 2 times more load than the reference sample. Cracks occurred in the horizontal joints on the left side of the vault and in the part where the load was applied in Model-1. The CFRP strips started to debond from the masonry unit in the area where the load was applied, starting from the keystone level.

Model-2 carried a higher load than Model-1 as CFRP strips were applied both inside and outside of the vault. The load-bearing capacity of Model-2 was measured at 31.335 kN. Model-2 had a vertical displacement of 4.110 mm and a horizontal displacement of 10.377 mm at maximum load. Model-2 carried 2 times more load than Model-1. In Model-2, the first cracks occurred in the interior at the level of the keystone when the load reached 20.12 kN. The CFRP in the interior of the vault was debonded from the surface at the level of the keystone and in the area where the load was applied. In the right part of the vault, large cracks were observed in the horizontal joints in the tension zone.

The biggest problem observed in CFRP applications in Model-1 and Model-2 was the debonding of CFRP strips over masonry units. At the same time, due to the application of CFRP strips from the starting point of the vault arc in these two samples, large cracks were observed in the regions where the vault arc began. To eliminate these deficiencies, anchoring was applied in Model-3 and Model-4. In Model-3, anchor holes with a diameter of 10 mm were drilled in three places, from the area where the load is applied to the inner part of the vault, one at two joint intervals. Anchors obtained by wrapping CFRP around 8 mm diameter and 40 mm long steel rods were placed in these drilled holes. Anchored Model-3 carried a maximum load of 33.898 kN. The vertical displacement of the Model-3 at its maximum carrying capacity was 3.727 mm, and the horizontal displacement was 9.315 mm. In Model-3, it was observed that the inner CFRP strips were debonded from the surface at the level of the keystone. No debonding or cracks were observed in the area where the anchors were made. Cracks were observed between the keystone where the anchor was not made and the concrete poured area. Large cracks occurred in the joint on the springer on the right outer part of the vault.

The maximum vertical load was carried by Model-4 test sample obtained by anchoring the inner and outer parts of the vault. This value was 40.822 kN. The vertical and horizontal displacement values of Model-4 under maximum load were 4.850 mm and 12.781 mm, respectively. Since CFRP strips were applied 150 mm below the springer in Model-3 and Model-4, no cracks were observed in the regions where the vault arc started. In Model-4, as a result of the experiment, cracks were observed in three anchorages in the inner part of the vault arc in the area where the load was applied. When Fig. 10 was examined, Model-4 exhibited the most ductile behavior among the vault tests.

Model-5, which was strengthened by tie rods, carried a maximum load of 12.171 kN. It had a vertical displacement of 7.973 mm and a horizontal displacement of 6.143 mm under maximum load. Large cracks occurred in the horizontal joints in the joint located next to the concrete pouring area where the load was applied and in the outer part of the vault arc.

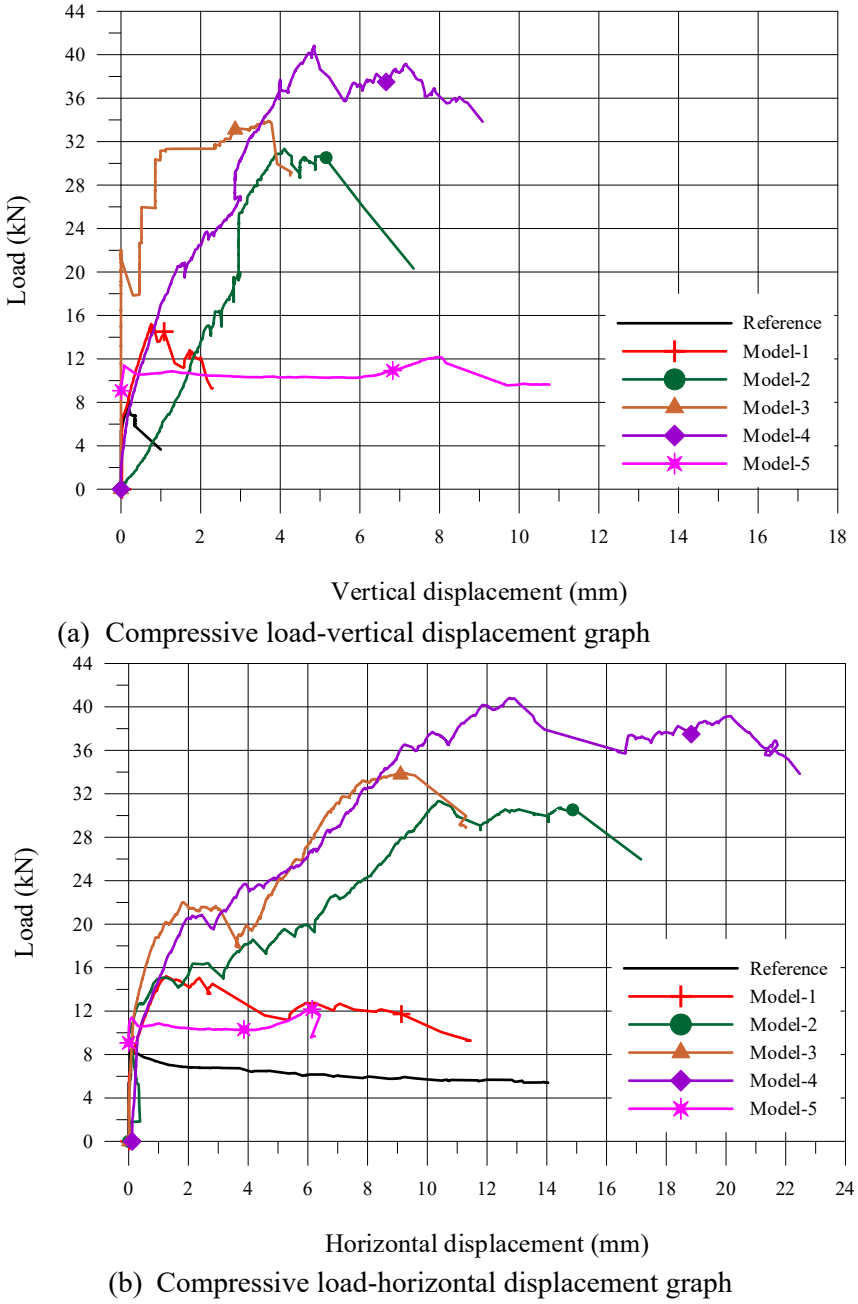

Fig. 10. a) Compressive load-vertical displacement graph, b) Compressive load-horizontal displacement graph.

4. Numerical analysis of vault samples

When the load–displacement graphs drawn as a result of the experimental studies were examined, the vault test samples showed a nonlinear behavior. For this reason, modelizing was analyzed considering the nonlinear properties of the materials. Numerical models of vault test samples were modeled in LUSAS [41] analysis program using the finite element method. Three different modeling techniques were used for modeling masonry units. These were Detailed Micro Modeling, Simplified Micro Modeling, and Macro Modeling.

The Poisson Ratio, elasticity modulus, and inelastic mechanical properties of stone and mortar forming masonry units in detailed micro-modeling were defined separately and analyzed. Based on detailed micro-modeling, it was assumed that cracks would form at the interface between the stone and the mortar. In the simplified micro modeling, the masonry units were expanded by half the thickness of the mortar, the mortar was neglected, and the masonry units were separated from each other by the interface. In this modeling, it was assumed that the cracks to occur would occur at the interfaces. In macro modeling, mortar and masonry units are homogenized and the masonry wall is considered a composite. In this modeling, the mechanical properties of the masonry wall obtained by homogenization are taken into account as mechanical properties. In this study, the macro modeling technique was applied. The properties of the materials were determined according to the tests performed on the masonry walls obtained. Linear and non-linear properties of the materials used in the analysis are given in Table 5.

The Drucker-Prager criterion, which represents the nonlinear behavior of masonry units, was used in the study. The Drucker-Prager criterion was made more sensitive to the hydrostatic state by adding a term to the Von-mises criterion used in steel-type materials and has become a criterion that can be used in masonry materials exhibiting brittle behavior. The Drucker-Prager criterion is expressed by Eq. (3).

Table 5
Material properties of the samples.

Material	Properties	Value
Upper concrete part	Young's modulus (MPa)	28,500
	Poisson's ratio	0.2
	Initial cohesion (MPa)	3
	Initial friction angle	33
	Slope of cohesion in tension	0.0
	Slope of friction in tension	0.0
	Plastic strain in tension	0.001
Homogenized masonry	Young's modulus (MPa)	1897
	Poisson's ratio	0.2
	Initial cohesion (MPa)	2.5
	Initial friction angle	25
	Slope of cohesion in tension	0.0
	Slope of friction in tension	0.0
	Plastic strain in tension	0.001
Steel tie rod	Young's modulus (MPa)	210,000
	Poisson's ratio	0.3
	Initial uniaxial yield stress (MPa)	275
	Hardening gradient slope in tension	212.1
	Plastic strain in tension	1.0
CFRP	Young's modulus (MPa)	25,000
	Poisson's ratio	0.3
	Initial uniaxial yield stress (MPa)	350

$$f(I_1, J_2) = \alpha I_1 + \sqrt{J_2} - k = 0 \tag{3}$$

The α and k are the positive material parameters in the equation, I_1 represents the first invariant of the tension tensor, and J_2 is the second invariant of the deviatoric tension tensor. When $\alpha = 0$, the equation gives the Von-Mises Equation. The Drucker-Prager fracture surface in the case of three-dimensional tension is shown in Fig. 11.

If the circle of the Drucker-Prager criterion, which is very close to the Mohr-Coulomb criterion, is considered as the circle drawn from the outside of the Mohr-Coulomb hexagon, the two surfaces 0 = 60° can be expressed by Eq. (4) in accordance with the basing meridian to be determined by α and k (Chen and Mizuno [42]). In the equation, ϕ and c represent the internal friction angle and cohesion, respectively.

$$\alpha = \frac{2\sin\phi}{\sqrt{3}(3 - sin\phi)}$$
$$k = \frac{6c\cos\phi}{\sqrt{3}(3 - sin\phi)} \tag{4}$$

At the same time, the constants that determine the inner cone with 0 = 0 passing through the tension meridian are found with Eq. (5).

$$\alpha = \frac{2\sin\phi}{\sqrt{3}(3 + \sin\phi)}$$
$$k = \frac{6c\cos\phi}{\sqrt{3}(3 + \sin\phi)} \tag{5}$$

In the numerical analysis of the vault models, the values of c = 2.5–3.70 MPa, Θ = 25–35 were used for the parameters Θ and c (Tugrulelci [43]). In the finite element models, three-dimensional solid elements are used for the masonry wall, tie rods, and also poured concrete to prevent the bricks from crushing on the upper surface of the vault. In the numerical model, three-dimensional tetrahedral solid elements with 10 node points and 3 degrees of freedom at each node were used (Fig. 12). Number of elements and node points used in the analysis of the vault samples are given in Fig. 13.

In the finite element analysis, as in the experimental study, a compressive load was applied to the vault models on the concrete poured at a distance of 230 mm from the keystone. The bottom ends of the pillars were designed as fully fixed support. The vertical load graphs corresponding to the vertical displacements under the keystone obtained as a result of the analysis and experimental study are given in Fig. 14, and the test and analysis results are given in Fig. 15. When the graphs are examined, it is seen that the test and analysis results behave close to each other as a general. But some small differences were observed in the behavior of numerical models in Model-2 and Model-4. It is thought that the reason for these differences is the uncertainties that

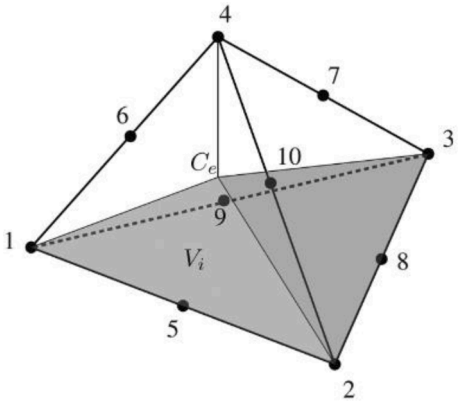

Fig. 12. Three-dimensional tetrahedral solid elements with 10 node points used in the analysis C_e; centroids, V_i; sub-volumes [44].

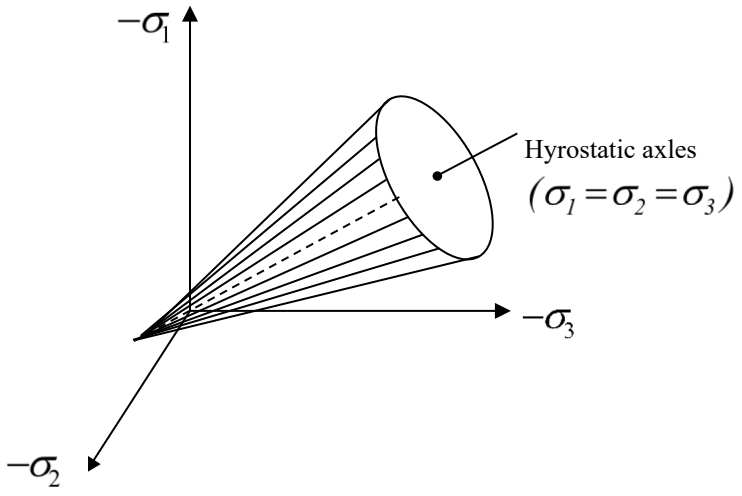

Fig. 11. Drucker-Prager kriteria (Chen and Mizuno [42]).

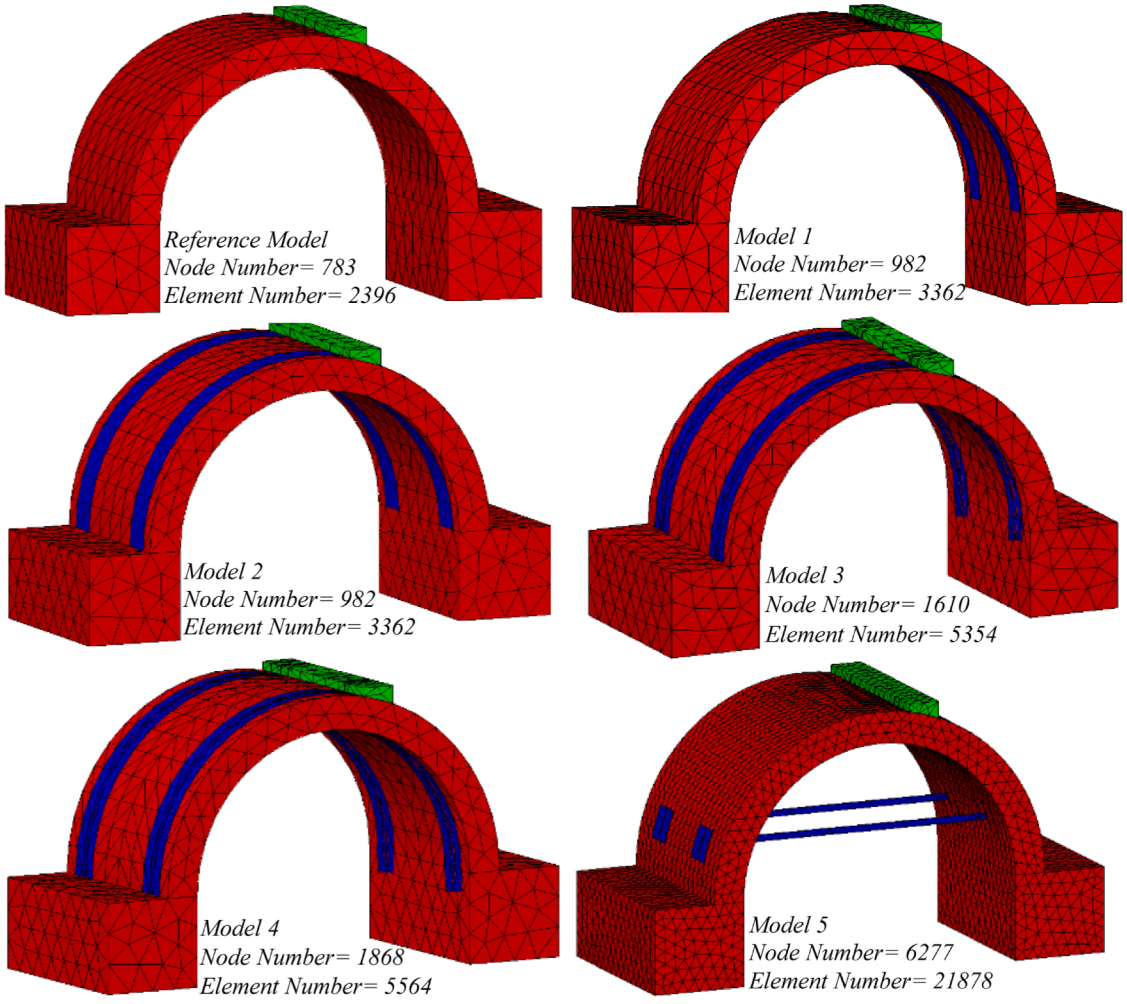

Fig. 13. Number of elements and node points used in the analysis of vault models.

can be seen in many civil engineering problems. Uncertainties in civil engineering problems are examined under two major titles as aleatory uncertainty and epistemic uncertainty. Aleatory uncertainty depends on basic variables (e.g., compressive strength of brick units and mortar, yield strength of tie rod) and cannot be changed. Epistemic uncertainty can be reduced with additional information and data. Epistemic uncertainties consist of statistical errors, modeling, and prediction errors. The loading rate in the experiment, the number of test samples, and the non-homogeneous structure/texture distribution of the bricks are all sources of epistemic uncertainty [45,46].

5. Conclusions

In this study, the behavior of six vault samples, one of which was the reference sample, one of which was reinforced with tie rods, and four of which were reinforced CFRP materials of different reinforcement techniques, were investigated experimentally and numerically under axial load. No strengthening method was applied in the sample called the reference. Two 100 mm wide CFRP strips were applied to the inside of the vault arc, leaving a 50 mm gap from the edges. This test sample was named Model-1. In Model-2, the vault sample was reinforced with two 100 mm wide CFRP strips, leaving 50 mm gaps from the both inner and outer parts. In the Model-3 test sample, as in Model-2, CFRP strip applications were made from the inner and outer parts of the vault. Unlike Model-2, CFRP strips were continued up to 150 mm below the springer (see Fig. 6a), and the anchorage was made to the inner part of the vault at a total of three points in two joint intervals on the area where the load was applied. The anchor was applied to both the inner and outer parts of the vault in Model-4, in a way that it would be two joint intervals. Finally, in Model-5, the vault sample was strengthened with tie rods. The tie rods were applied from the 60 % lower part of the vault height, where the tensile strength of the vault was formed. The tie rods were fixed to the 10 mm thick square plate with the help of bolts. The samples mentioned above were tested by applying a vertical load corresponding to 1/4 of the vault span. When the experimental results and numerical analysis results were compared, it was seen that the results were close to each other. The results obtained as a result of the study are summarized below.

- The load-bearing capacity of the reinforced samples increased by at least 45 % compared to the unreinforced reference sample.
- Model-1, which was reinforced with CFRP strips only from the inside of the vault, carried 81.49 % more load than the reference sample. In Model-1, it was observed that the CFRP strips were debonded over the masonry units with the increase in the load, and there were wide cracks at the horizontal joints on the outer part of the vault and at the area where the vault arc began.
- To prevent the cracks of the horizontal joints on the outer part of the vault seen in Model-1, Model-2 test sample was made. In Model-2 by wrapping the outer part with additional CFRP strips, the load-bearing capacity increased in the percentage of 106. In addition,

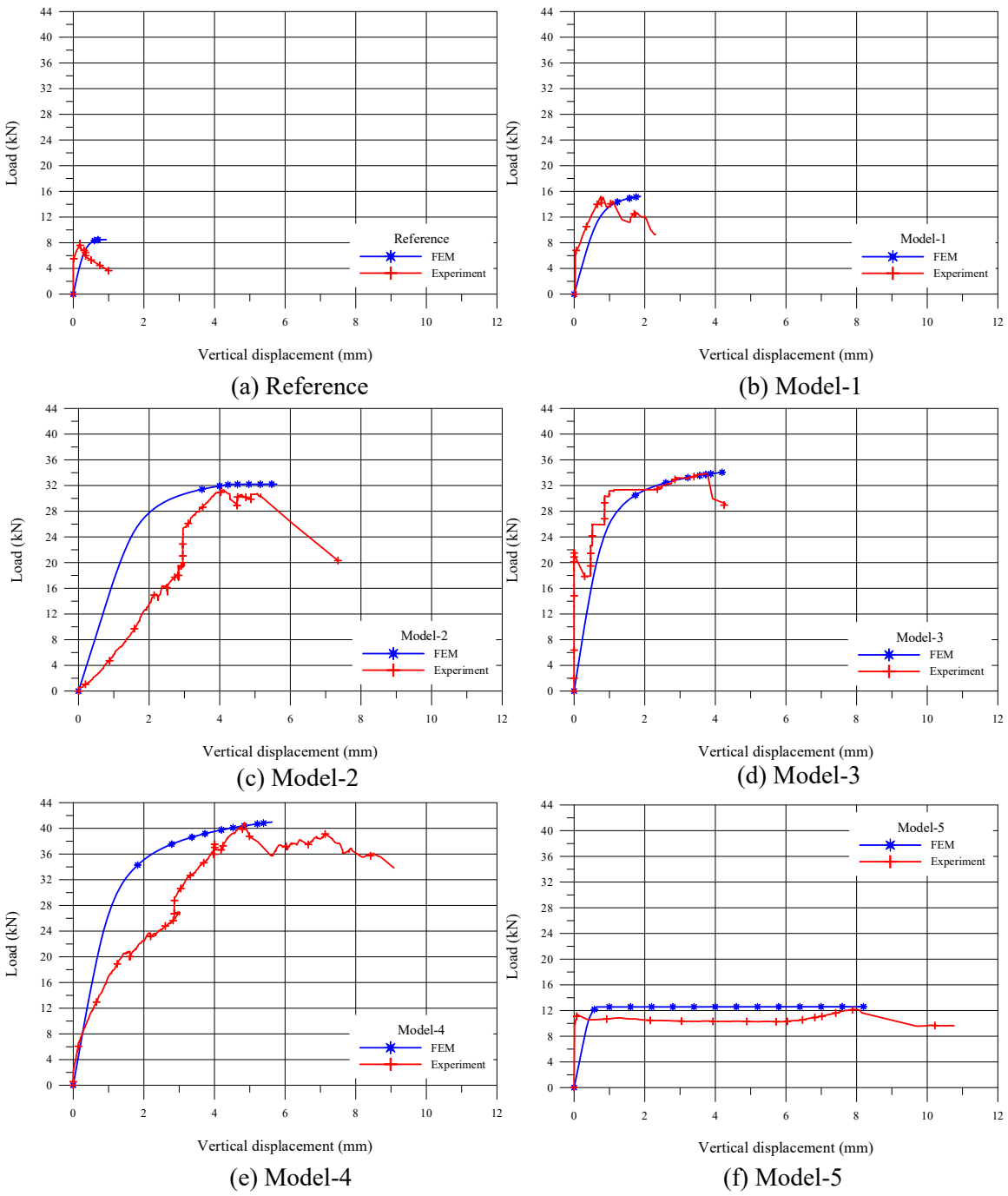

Fig. 14. Comparing finite elements and compressive load-vertical displacement graphs obtained from the test results.

the vertical and horizontal displacements of Model-2 under maximum load were higher than Model 1.

- Among the vault test samples reinforced in different ways, Model-4 carried the highest load. To prevent cracks seen on the area where the vault arc began in Model-1 and Model-2, CFRP strips in Model-3 and Model-4 were continued up to 150 mm below the springer. According to the test results, cracks on the springers were not observed. In addition, the anchors applied prevented the debonding of CFRP strips from the masonry units and increased the load-bearing capacity, allowing the structure to exhibit a more ductile behavior.
- In Model-3, three anchors were applied to the lower part of the point where the load was applied. Model-3 carried 16.96 % less load than Model-4. The reason why it carries less load compared to Model-4 was that the anchor was made in certain areas and the inner part. As a result of the experiment, it was observed that no cracks were observed in the anchored areas, and in the non-anchored areas, the CFRP strips were debonded from the masonry units.
- The test sample that carried the least load was Model-5, which was reinforced with tie rods. The load-bearing capacity of Model-5 increased by 45 % compared to the reference sample. On the other hand, the sample reinforced with tie rods showed more ductile behavior than the reference sample.

At the end of this study, it was determined that CFRP materials increased the load-bearing capacity in the repair and strengthening works, prevented the development of hinges that occurred in four places

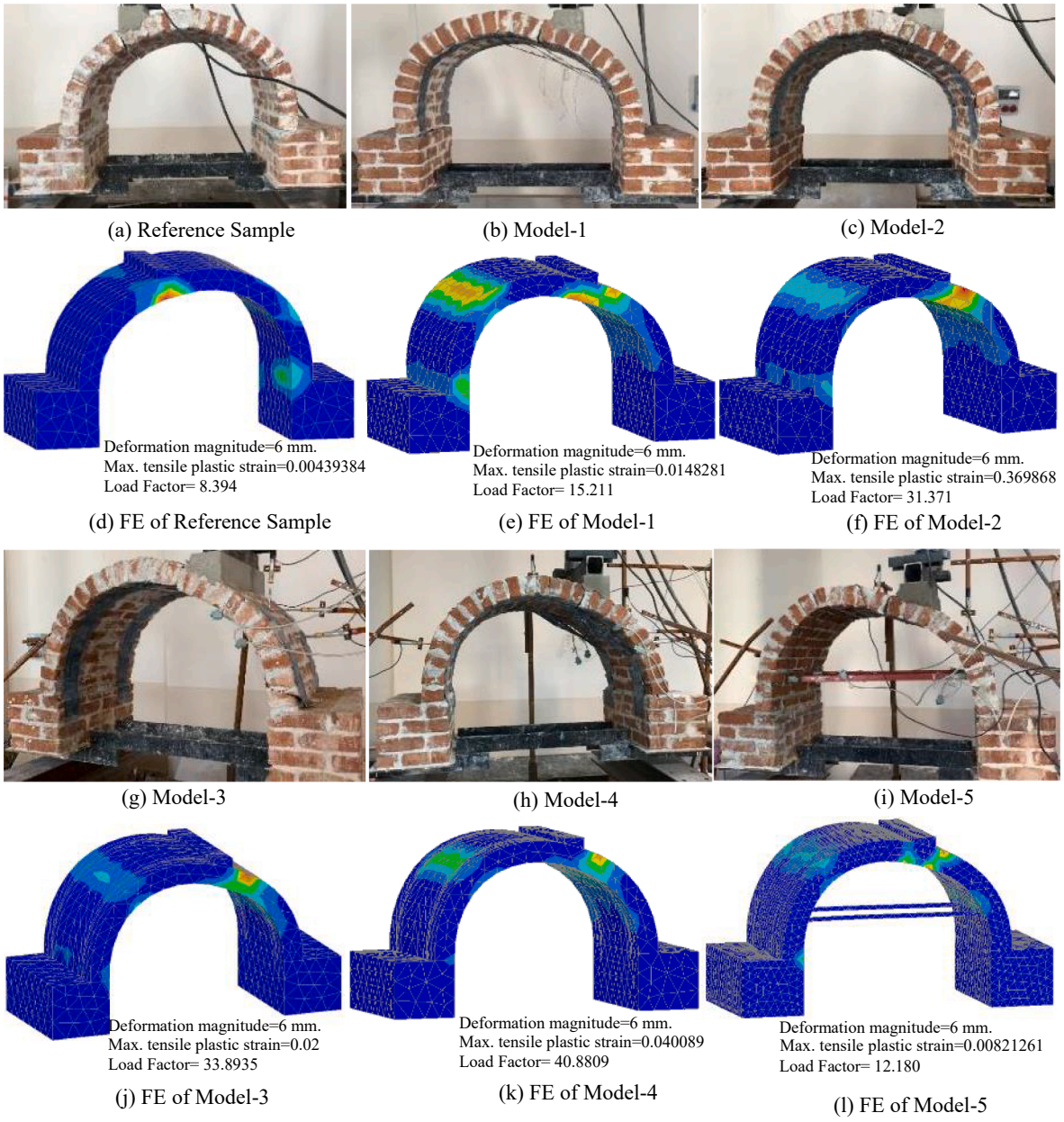

Fig. 15. Experiment and analysis results.

in the vaults, and decreased damage intensification. The anchoring application showed that the CFRP strips used are not debonded from the masonry units and increased the load-bearing capacity. Besides, it was determined that CFRP strips should be continued up to the bottom of the springer, where the vault arc begins, in the repair and strengthening of the vaults.

Declaration of Competing Interest

The authors declare that they have no known competing financial interests or personal relationships that could have appeared to influence the work reported in this paper.

Acknowledgment

This study was supported by Aksaray University Scientific Research Projects (Project no: 2022/026).

References

[1] Tarhan İH. "Investigation by finite element method of masonry vaults that reinforced with composites. Master's Thesis'' 2018.
[2] Bernardeschi K, Padovani C, Pasquinelli G. Numerical modelling of the structural behaviour of Buti's bell tower. J Cult Herit 2004;5(4):371–8. https://doi.org/10.1016/j.culher.2004.01.004.
[3] Calderini C, Chiorino MA, Lagomarsino S, Spadafora A. Non linear modelling of the elliptical dome of Vicoforte. Structural Analysis of Historical Constructions: New Delhi; 2006. p. 1177–86.
[4] De Stefano A. Structural identification and health monitoring on the historical architectural heritage. Key Eng Mater 2007;347:37–54. https://doi.org/10.4028/www.scientific.net/KEM.347.37.
[5] Ural A, Firat FK. Evaluation of masonry minarets collapsed by a strong wind under uncertainty. Nat Hazards 2015;76(2):999–1018. https://doi.org/10.1007/s11069-014-1531-7.
[6] Rossi M, Barentin CC, Van Mele T, Block P. Experimental study on the behaviour of masonry pavilion vaults on spreading supports. Structures 2017;11:110–20. https://doi.org/10.1016/j.istruc.2017.04.008.
[7] Aghabeigi P, Tabar SF. Seismic vulnerability assessment and retrofitting of historic masonry building of Malek Timche in Tabriz Grand Bazaar. Eng Struct 2021;240:112418. https://doi.org/10.1016/j.engstruct.2021.112418.

[8] Altunişik AC, Sunca F, Genç AF, Tavşan C. Post-Earthquake damage assessments of historic mosques and effects of near-fault and far-fault ground motions on seismic responses. Int J Arch Heritage 2021:1–36. https://doi.org/10.1080/15583058.2021.2011475.
[9] Buyukkaragoz A, Kopraman Y. In-plane behaviour of masonry brick walls strengthened with mortar from two sides. Structures 2021;29:1627–39. https://doi.org/10.1016/j.istruc.2020.12.029.
[10] Hejazi M, Baranizadeh S, Daei M. Performance of Persian brick masonry single-shell domes subjected to uniform pressure and concentrated load. Structures 2021;34:1710–9. https://doi.org/10.1016/j.istruc.2021.08.100.
[11] Jasieńko J, Raszczuk K, Kleszcz K, Frąckiewicz P. Numerical analysis of historical masonry domes: A study of St. Peter's Basilica dome Struct 2021;31:80–6. https://doi.org/10.1016/j.istruc.2021.01.082.
[12] Jing DH, Krevaikas T, Zhang H. Pre-stressed steel strips for the strengthening of axially loaded masonry walls. Structures 2021;30:25–40. https://doi.org/10.1016/j.istruc.2021.01.001.
[13] Tanrıverdi Ş., "Investigation of the effects of window opening and pulley height on behavior and strength on stone domes, Ph.D. Thesis'' 2020.
[14] Usta P. Assessment of seismic behavior of historic masonry minarets in Antalya. Turkey Case Stud Constr Mater 2021;15:e00665.
[15] D'Altri AM, De Miranda S, Castellazzi G, Sarhosis V, Hudson J, Theodossopoulos D. Historic barrel vaults undergoing differential settlements. Int J Arch Heritage 2019;14(8):1196–209. https://doi.org/10.1080/15583058.2019.1596332.
[16] Yurdakul M, Yılmaz F, Artar M, Can Ö, Öner E, Daloğlu AT. Investigation of time-history response of a historical masonry minaret under seismic loads. In Structures 2021;30:265–76. https://doi.org/10.1016/j.istruc.2021.01.008.
[17] Fırat FK, Ural A, Kara ME. January 24, 2020 Sivrice Earthquake and the response of the masonry Haci Yusuf Tas (New) mosque. Earthquakes and Structures, 2022;22(4):331. https://doi.org/10.12989/eas.2022.22.4.331.
[18] Mercuri M, Pathirage M, Gregori A, Cusatis G. Masonry vaulted structures under spreading supports: Analyses of fracturing behavior and size effect. J Build Eng 2022;45:103396. https://doi.org/10.1016/j.jobe.2021.103396.
[19] Foraboschi P. Strengthening of masonry arches with fiber-reinforced polymer strips. J Compos Constr 2004;8(3):191–202. https://doi.org/10.1061/(ASCE)1090-0268(2004)8:3(191).
[20] Milani G, Bucchi A. Kinematic FE homogenized limit analysis model for masonry curved structures strengthened by near surface mounted FRP bars. Compos Struct 2010;93:239–58. https://doi.org/10.1016/j.compstruct.2010.05.013.
[21] Fırat FK, Eren A. Investigation of FRP effects on damaged arches in historical masonry structures. J Fac Eng Archit Gazi Univ 2015;30(4):659–70. https://doi.org/10.17341/gummfd.46980.
[22] Ural A, Fırat FK, Tuğrulelçi Ş, Kara ME. Experimental and numerical study on effectiveness of various tie-rod systems in brick arches. Eng Struct 2016;110:209–21. https://doi.org/10.1016/j.engstruct.2015.11.038.
[23] Carozzi FG, Poggi C, Bertolesi E, Milani G. Ancient masonry arches and vaults strengthened with TRM, SRG and FRP composites: Experimental evaluation. Compos Struct 2018;187:466–80. https://doi.org/10.1016/j.compstruct.2017.12.075.
[24] De Santis S, Roscini F, De Felice G. Full-scale tests on masonry vaults strengthened with Steel Reinforced Grout. Compos B Eng 2018;141:20–36. https://doi.org/10.1016/j.compositesb.2017.12.023.
[25] Hamdy G, Kamal O, Al-Hariri O, El-Salakawy T. Plane and vaulted masonry elements strengthened by different techniques–testing, numerical modeling and nonlinear analysis. J Build Eng 2018;15:203–17. https://doi.org/10.1016/j.jobe.2017.11.009.
[26] Zampieri P, Simoncello N, Tetougueni CD, Pellegrino C. A review of methods for strengthening of masonry arches with composite materials. Eng Struct 2018;171:154–69. https://doi.org/10.1016/j.engstruct.2018.05.070.
[27] De Santis S, De Felice G, Roscini F. Retrofitting of masonry vaults by basalt textile-reinforced mortar overlays. Int J Arch Heritage 2019;13(7):1061–77. https://doi.org/10.1080/15583058.2019.1597947.
[28] Varro R, Bögöly G, Görög P. Laboratory and numerical analysis of failure of stone masonry arches with and without reinforcement. Eng Fail Anal 2021;123:105272. https://doi.org/10.1016/j.engfailanal.2021.105272.
[29] Alejo Guerra, LE., "Seismic behaviour and strengthening of barrel vaults of Augustinian churches in Mexico, Ph.D. Thesis'' 2022.
[30] Siha A, Zhou C. Experimental investigation of axial compression in composite strengthened historical timber columns. Int J Arch Heritage 2022:1–18. https://doi.org/10.1080/15583058.2022.2039975.
[31] Firat FK, Kayabaşı MS. Investigation of tie-rod connection types on stone masonry arches. In Structures 2022;45:2185–97. https://doi.org/10.1016/j.istruc.2022.10.044.
[32] EN 772-1:2011+A1. Methods of test for masonry units - Part 1: Determination of compressive strength, Turkish Standard, Ankara, Turkey, 2015.
[33] EN 772-6. Methods of test for masonry units - Part 6: Determination of bending tensile strength of aggregate concrete masonry units, Turkish Standard, Ankara, Turkey, 2004.
[34] EN 12390-3. Testing hardened concrete - Part 3: Compressive strength of test specimens, Turkish Standard, Ankara, Turkey, 2019.
[35] EN 12390-6. Testing hardened concrete - Part 6: Tensile splitting strength of test specimens, Turkish Standard, Ankara, Turkey, 2010.
[36] EN ISO 6892-1. Metallic materials-Tensile testing- Part 1: Method of test at room temperature, todu, Turkish Standard, Ankara, Turkey, 2020.
[37] Kara ME, Firat FK, Sonmez M, Karabork T. An investigation of anchorage to the edge of steel plates bonded to RC structures. Steel Compos Struct 2016;2(1):25–43. https://doi.org/10.12989/scs.2016.22.1.025.
[38] EN 1052-1:1998. Methods of test for masonry - Part 1: Determination of compressive strength, Turkish Standard, Ankara, Turkey, 2000.
[39] EN 1996-1-1+A1. Design of masonry structures-Part 1-1: General rules for reinforced and unreinforced masonry structures, Turkish Standard, Ankara, Turkey, 2013.
[40] Valluzzi MR, Valdemarca M, Modena C. Behavior of brick masonry vaults strengthened by FRP laminates. J Compos Constr 2001;5(3):163–9. https://doi.org/10.1061/(ASCE)1090-0268(2001)5:3(163).
[41] Lusas. Finite element analysis software products. United Kingdom: finite element system. FEA Ltd.; 2020.
[42] Chen WF, Mizuno E. Nonlinear Analysis in Soil Mechanics. Elsevier Science Publishers B.V; 1990.
[43] Tuğrulelçi Ş. "The examination of behaviour of vertical loaded brick masonry arch having tie rods. Master's Thesis'' 2014.
[44] Bilotta A, Turco E. (2017). Elastoplastic analysis of pressure-sensitive materials by an effective three-dimensional mixed finite element. ZAMM-Journal of Applied Mathematics and Mechanics/Zeitschrift für Angewandte Mathematik und Mechanik, 2017;97(4):382-396. http://doi.org/10.1002/zamm.201600051.
[45] Firat FK, Yucemen MS. Determination of new load and resistance factors for reinforced concrete structural members. Teknik Dergi 2014:1785–808.
[46] Firat FK, Yucemen MS. Comparison of loads in Turkish earthquake code with those computed statistically. Earthquakes Struct 2015;8(5):977–94. https://doi.org/10.12989/eas.2015.8.5.977.